



# Preparation and in vitro evaluation of $^{177}\text{Lu}$ -iPSMA-RGD as a new heterobivalent radiopharmaceutical

Alondra Escudero-Castellanos<sup>1,2</sup> · Blanca E. Ocampo-García<sup>1</sup> ·  
Guillermina Ferro-Flores<sup>1</sup> · Keila Isaac-Olivé<sup>2</sup> · Clara L. Santos-Cuevas<sup>1</sup> ·  
Andrea Olmos-Ortiz<sup>3</sup> · Janice García-Quiroz<sup>4</sup> · Rocío García-Becerra<sup>4</sup> ·  
Lorenza Díaz<sup>4</sup>

Received: 29 August 2017 / Published online: 20 October 2017  
© Akadémiai Kiadó, Budapest, Hungary 2017

**Abstract** This study aimed to synthesize a new  $^{177}\text{Lu}$ -iPSMA-RGD heterobivalent radiopharmaceutical, as well as to assess the in vitro radiopharmaceutical potential to target cancer cells overexpressing PSMA and  $\alpha(v)\beta(3)$  integrins. The radiotracer prepared with a radiochemical purity of  $98.8 \pm 1.0\%$  showed stability in human serum, specific recognition with suitable affinity to PSMA and  $\alpha(v)\beta(3)$  integrins, and capability to inhibit cancer cell proliferation and VEGF signaling (antiangiogenic effect). Results warrant further preclinical studies to establish the  $^{177}\text{Lu}$ -iPSMA-RGD potential as a dual therapeutic radiopharmaceutical.

**Keywords** PSMA inhibitor · RGD peptide ·  $^{177}\text{Lu}$  ·  $^{177}\text{Lu}$ -labeled PSMA inhibitor ·  $^{177}\text{Lu}$ -labeled RGD · Heterobivalent radiopharmaceutical

## Introduction

The prostate specific membrane antigen (PSMA) is expressed in normal prostate epithelial cells but is overexpressed in 95% of metastatic prostate cancers (mPCa) [1]. That is why the PSMA protein is an appropriate molecular target for imaging and radiotherapy of mPCa using specific radiopharmaceuticals [2, 3]. However, PSMA is a multifunctional protein, as it can act as an internalization receptor, as a nutrient absorption enzyme, or as a peptidase involved in signal transduction in epithelial cells and cell migration [4]. Thus, radiopharmaceuticals based on PSMA inhibitors (iPSMA) can also be used in other types of neoplasia different than mPCa, such as differentiated thyroid cancer, gliomas, metastatic breast cancer, and osteosarcomas, among others [5–8].

Radiopeptides based on the Arg-Gly-Asp (RGD) sequence show high affinity and selectivity for the  $\alpha(v)\beta(3)$  integrins. As a result, these peptides are useful for targeting tumors due to the overexpression of integrins in the tumor neovasculature and lung carcinoma, neuroblastoma, glioblastoma, osteosarcoma, melanoma, and breast cancer tumor cells [9, 10].

The research on new heterobivalent radiopharmaceuticals that interact with two different targets on tumor cells is a strategy for the enhancement of tumor imaging and therapy [11–13]. Therefore, a heterobivalent conjugate of iPSMA and RGD is expected to improve the recognition of cancer cells positive for PSMA and  $\alpha(v)\beta(3)$  integrins.

The aim of this study was to synthesize the Glu-CO-Lys-Nal-Cys(cRGDFK(MP))-DOTA- $^{177}\text{Lu}$  ( $^{177}\text{Lu}$ -iPSMA-RGD) heterobivalent radioconjugate, as well as to assess its in vitro potential to target C6 and U87MG cells overexpressing PSMA and  $\alpha(v)\beta(3)$  integrins.

✉ Blanca E. Ocampo-García  
blanca.ocampo@inin.gob.mx; ocampo\_be@yahoo.com.mx

<sup>1</sup> Departamento de Materiales Radiactivos, Instituto Nacional de Investigaciones Nucleares, Carretera México-Toluca S/N, 52750 Ocoyoacac, Estado de México, Mexico

<sup>2</sup> Facultad de Medicina, Universidad Autónoma del Estado de México, Paseo Tolloacan S/N, 50180 Toluca, Estado de México, Mexico

<sup>3</sup> Departamento de Inmunobioquímica, Instituto Nacional de Perinatología Isidro Espinosa de los Reyes, Montes Urales No. 800, Lomas de Virreyes, 11000 Ciudad de México, Mexico

<sup>4</sup> Departamento de Biología de la Reproducción, Instituto Nacional de Ciencias Médicas y Nutrición Salvador Zubirán, Av. Vasco de Quiroga 15, 14080 Ciudad de México, Mexico

## Experimental

### Synthesis of iPSMA-RGD

The iPSMA-RGD (((5-(2-(3-((1-(4-((4-((2S,5S,11S,14R)-14-benzyl-11-(carboxymethyl)-5-(3-guanidinopropyl)-3,6,9,12,15-pentaoxo-1,4,7,10,13-pentaaazacyclo-pentadecan-2-yl) butyl)amino)-4-oxobutyl)-2,5-dioxopyrrolidin-3-yl)thio)-2-(2-(4,7,10-tris(carboxymethyl)-1,4,7,10-tetraazacyclododecan-1-yl)acetamido)propanamido)-3-(naphthalen-2-yl) propanamido)-1-carboxypentyl)carbamoyl)glutamic acid) (MW 1775.37 g/mol) peptide (Fig. 1A) was designed at ININ (Instituto Nacional de Investigaciones Nucleares, Mexico) and synthesized with the support of Ontores Biotechnology Co., Ltd (Zhejiang, China). Briefly, the Glu-CO-Lys sequence was first obtained as previously reported [2]. The peptide synthesis continued by addition of Fmoc- $\beta$ -naphthyl alanine, Fmoc-cysteine(tBu) and DOTA (1,4,7,10-tetraazacyclododecane-N, N', N'', N'''-tetraacetic acid) to form the Glu-CO-Lys-Nal-Cys-DOTA sequence following the standard solid-phase peptide synthesis protocols (SPPS) [14]. The cyclo(Arg-Gly-Asp-DPhe-Lys(maleimidepropionyl)) (cRGDfK(MP)) was synthesized as reported elsewhere [15], with the difference being the use of D-Phe instead of D-Tyr. Finally, MP from the cRGDfK(MP) molecule was used as the crosslinking site to react with the cysteine sulfhydryl group of Glu-CO-Lys-Nal-Cys-DOTA

in order to obtain the Glu-CO-Lys-Nal-Cys(cRGDfK(MP))-DOTA conjugate (iPSMA-RGD) (Fig. 1). The molecular structure was characterized by IR (ATR-FTIR), mass (MALDI as ionization technique) [ $m/z$  [MALDI + 2H] $^{2+}$  = 888.6, [M + H] $^{+}$  (calc. 887.6)] and UV spectroscopies. The chemical purity was > 98%, as determined by reversed phase HPLC (RP-HPLC) (Fig. 1). The peptide eluted at  $t_R$  = 9.14 min from an analytical HPLC column, using a water/acetonitrile gradient containing 0.1 and 0.08% TFA from 95/5 to 10/90 in 30 min at a flow rate of 1 mL/min (room temperature).

### Labeling of iPSMA-RGD with Lu-177

To 100  $\mu$ L of a solution of iPSMA-RGD (0.5 mg in 1 mL of 0.2 M acetate buffer, pH 5), 50  $\mu$ L (740 MBq) of  $^{177}\text{LuCl}_3$  (> 3 TBq/mg, EndolucinBeta $^{\text{®}}$ , ITG, Germany) were added. The mixture was placed in a block heater at 95  $^{\circ}\text{C}$  for 30 min. The final solution was diluted to 1 mL with a solution of ascorbic acid (10 mg/mL). For comparative studies, the DOTA-cyclo-RGDfK (Pichem, Austria) synthesized as previously reported [10] and DOTA-PSMA-617 (ABX, Germany) were also radiolabeled under the same procedure.

Radiochemical purity was evaluated on a reversed-phase high-performance liquid chromatography (HPLC) system (Waters, USA) equipped with UV and radioactivity

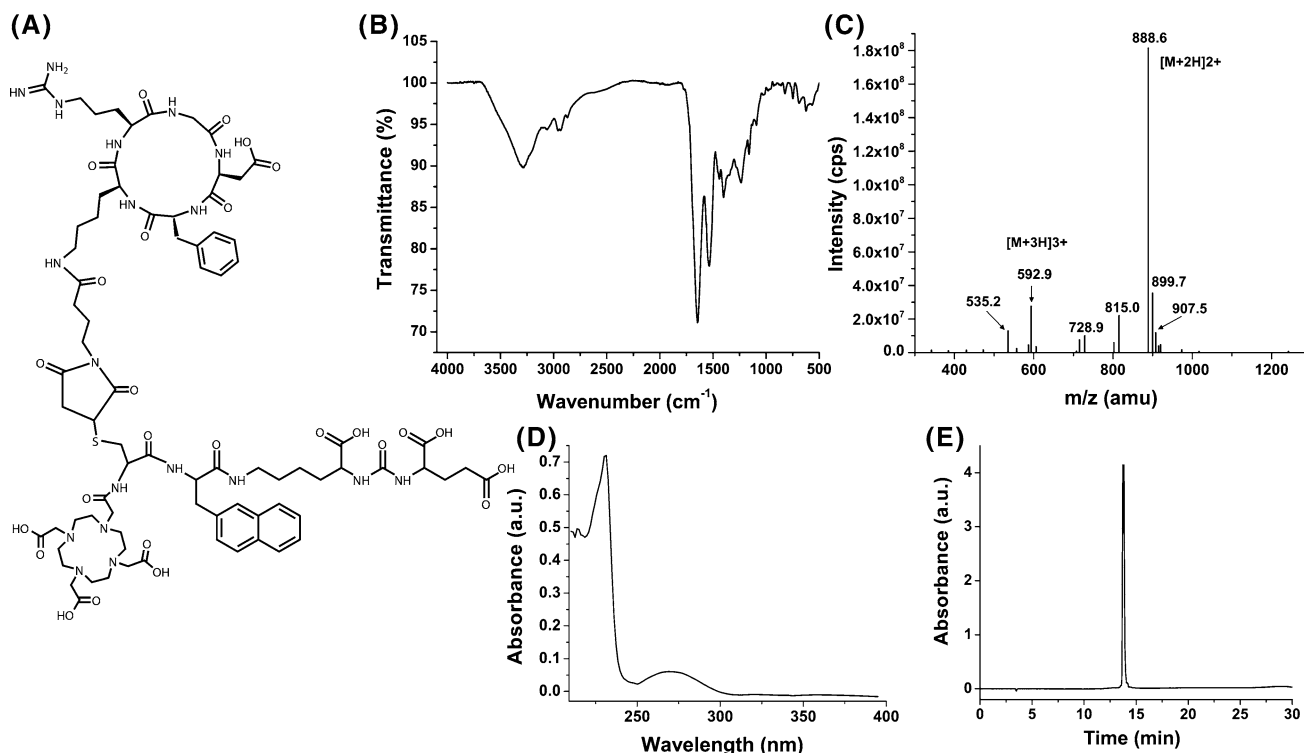


**Fig. 1** A Schematic structure of the synthesized iPSMA-RGD and its chemical characterization by B IR (ATR-FTIR), C mass (MALDI as ionization technique), D UV-Vis spectroscopies and E Reversed-phase HPLC analysis

detectors. Analyses were performed using an analytical C18 column ( $\mu$ Bondapak 5  $\mu$ m,  $3.9 \times 300$  mm<sup>2</sup>) under a linear gradient of water/acetonitrile containing 0.1% of TFA from 98/5 to 2/90 in 30 min at a flow rate of 1 mL/min. The retention time for <sup>177</sup>LuCl<sub>3</sub> was  $3.6 \pm 0.3$  and  $15.6 \pm 0.3$  min,  $14.1 \pm 0.3$  and  $15.3 \pm 0.3$  min for <sup>177</sup>Lu-iPSMA-RGD, <sup>177</sup>Lu-DOTA-cyclo-RGDfK (<sup>177</sup>Lu-RGD) and <sup>177</sup>Lu-DOTA-PSMA-617 (<sup>177</sup>Lu-iPSMA), respectively.

### Serum stability

For the stability evaluation of the radiopeptides in serum, an analytical size-exclusion HPLC column (ProteinPak 300SW Waters) at a 1 mL/min flow rate and 0.01 M PBS as eluent was used. <sup>177</sup>Lu-iPSMA-RGD was incubated with 2 mL of diluted (1:10) human serum at 37 °C. Samples (30  $\mu$ L) were taken at different times (from 30 min to 24 h) for radio-HPLC analysis.

### In vitro cell studies

#### Cell culture

C6 (RGD-positive) rat brain glioma cells (ATCC<sup>®</sup> CCL-107<sup>TM</sup>), U87MG (RGD-positive) human primary glioblastoma cell line (ATCC<sup>®</sup> HTB-14<sup>TM</sup>) and EA.hy926 endothelial cells (ATCC<sup>®</sup> CRL-2922<sup>TM</sup>) were originally obtained from ATCC (USA). The cells were routinely grown at 37 °C in an incubator with humidified air (85% humidity), 5% CO<sub>2</sub> and cultured in Roswell Park Memorial Institute Medium (RPMI, Sigma-Aldrich Co.), supplemented with antibiotics (100  $\mu$ g/mL streptomycin and 100 U/mL penicillin) and 10% fetal bovine serum.

#### Cell binding affinity

<sup>177</sup>Lu-iPSMA-RGD binding affinity was determined by a competitive cell binding assay. Briefly, C6 or U87MG cells ( $1 \times 10^5$  per well) were incubated at 37 °C in 96-well cell culture plates for 24 h. Then, cells were incubated at 37 °C for 1 h with “cold” peptides (iPSMA and/or RGD) at 8 different concentrations (from 10,000 to 0.01 nM, 30  $\mu$ L/well,  $n = 3$ ) in the presence of a constant concentration of <sup>177</sup>Lu-iPSMA-RGD (0.2 nM, 100  $\mu$ L, 10 kBq). After incubation, the supernatant was removed, and the cells were washed three times with cold binding buffer (25 mM Tris-HCl, 1 mM CaCl<sub>2</sub>, 150 mM NaCl, 0.1% bovine serum albumin, pH 7.4). The radioactivity of each well was counted in a gamma NaI(Tl) detector (NML Inc., USA), which represented the cell-bound activity. The initial activity of each treatment was determined by the previous preparation of a standard representing 100%. The 50%

inhibitory concentration (IC<sub>50</sub>) was calculated by fitting the competitive binding curves using a nonlinear regression analysis (Origin8 Software). The same procedure was performed to determine IC<sub>50</sub> values for <sup>177</sup>Lu-iPSMA and <sup>177</sup>Lu-RGD.

#### Saturation assay

C6 or U87MG cells ( $8 \times 10^4$  per well) were incubated in 48-well cell culture plates for 24 h. Then, cells were incubated at 4 °C for 1 h with <sup>177</sup>Lu-iPSMA-RGD at eight different concentrations (from 1000 to 0.01 nM, 120  $\mu$ L/well plus 30  $\mu$ L of binding buffer,  $n = 3$ ). The non-specific binding was determined in parallel by addition of 30  $\mu$ L of the non-radiolabeled analog (2  $\mu$ M <sup>176</sup>Lu-iPSMA-RGD, prepared by using 82.8% enriched <sup>176</sup>Lu, Isoflex, USA) instead of the 30  $\mu$ L of the binding buffer. After incubation, the supernatant was removed, the cells were washed three times with 100  $\mu$ L cold binding buffer, and the radioactivity of the total withdrawn volume was counted in a gamma NaI(Tl) detector (NML Inc., USA), which represented the non-cell-bound activity. The initial radioactivity of each treatment was determined by the previous preparation of standards representing 100%. The cell bound radioactivity corresponds to the activity measurement of the cells collected with 1 M NaOH. Specific binding was calculated as the difference between total binding and non-specific binding.  $B_{\max}$  and  $K_d$  were determined by nonlinear regression analysis (GraphPad Prism software). The same procedure was followed to calculate the  $B_{\max}$  and  $K_d$  values for <sup>177</sup>Lu-iPSMA and <sup>177</sup>Lu-RGD.

#### Cell uptake

U87MG or C6 cells were harvested and diluted in fresh medium ( $1 \times 10^5$  cells/well, 0.5 mL) to then be seeded in 48-well tissue culture plates. After 24 h, the medium was removed, and the cells were incubated with a 25 nM solution of each treatment (<sup>177</sup>Lu-iPSMA-RGD, <sup>177</sup>Lu-iPSMA or <sup>177</sup>Lu-RGD, 30  $\mu$ L/well, 100  $\mu$ L of phosphate-buffered saline) for 45 min at 37 °C. Then, two rinses were performed with one mL of ice-cold phosphate-buffered saline (PBS). The cells were washed twice with 0.5 mL of 1 M NaOH (fraction of cell uptake and radiotracer internalization). Radioactivity was measured in a NaI(Tl) detector (NML Inc. USA). The initial activity of each treatment was taken to represent 100%. In parallel, the non-specific binding was determined using 250  $\mu$ M of iPSMA-RGD, PSMA-617 or cRGDfK, which blocked cell receptors.

### Cell viability assay

The effect of  $^{177}\text{Lu}$ -iPSMA-RGD,  $^{177}\text{Lu}$ -iPSMA or  $^{177}\text{Lu}$ -RGD treatments on cell viability was assessed by the mitochondrial dehydrogenase activity in living C6 or U87MG cells by using the XTT (2, 3-bis[2-Methoxy-4-nitro-5-sulphophenyl]-2H-tetrazolium-5-carboxyanilide inner salt; 0.1 mg/mL) assay kit (Roche, Germany). Briefly, C6 cells were seeded in 96-well microtiter plates ( $8 \times 10^3$  cells/well) and incubated overnight to allow cell attachment. The growth medium was removed, and the cells were incubated for 4 h with approximately 2 kBq/cell of each treatment (200  $\mu\text{L}$ ). The viability after exposure to the treatment was evaluated 24 h and 48 h (37 °C, 5%  $\text{CO}_2$ , and 85% humidity). The cell proliferation percentage in each well was evaluated by the spectrophotometric measurement of cell viability (absorbance of the orange solution) at 450 nm in a microplate absorbance reader (Epoch<sup>TM</sup>, BioTek Instruments, USA). The untreated cell absorbance was considered as 100% viability.

### Western blot (inhibition of VEGF signaling)

After a serum fasting overnight, EA.hy926 endothelial cells were exposed during 3 h to 200  $\mu\text{M}$   $\text{CoCl}_2$  (hypoxia-like conditions). Then cells were treated with “cold” iPSMA or iPSMA-RGD for 5 min in the presence of serum. Culture medium with and without serum were used as positive and negative control, respectively. Cells were then lysed (HEPES 50 mM, NaCl 250 mM, EDTA 5 mM, NaF 10 mM, Nonidet P-40 0.1%,  $\beta$  glycerophosphate 50 mM,  $\text{Na}_3\text{VO}_4$  1 mM, pH 7.4). Proteins were separated by SDS-PAGE 10%, transferred to a Hy-bond ECL nitrocellulose membrane (Amersham) and blocked for 1 h at room temperature (skim milk 5% in TBS-tween 0.05%). Membranes were incubated overnight at 4 °C in the presence of the rabbit monoclonal antibody anti-pVEGFR2 (Cell Signaling Technology, D5B11, 1:2000 in TBS-T 0.05% + 1% BSA), which identifies phosphorylated VEGFR2 in Y1175, followed by incubation with the secondary antibody HRP-goat anti-rabbit (Zymed, 65–6120) 1:10,000 in TBS-T 0.05% for 1 h at room temperature. Load control was evaluated with actin detection (goat polyclonal anti-actin (Santa Cruz, sc-1616) 1:3000 in TBS-T 0.05 + 3% skim milk overnight at 4 °C, followed by incubation with secondary antibody HRP-rabbit anti-goat (Thermo, 31210) 1:30,000 in TBS-T 0.05% for 1 h at room temperature. The proteins were visualized by using the ECL-Plus western blotting detection system (GE Healthcare, UK), using the Bio-Rad ChemiDoc XRS detection system (Bio-Rad Hercules, CA).

### Statistical analysis

Data were expressed as mean  $\pm$  SD of the results of three independent replicas of each assayed condition. Differences between treatments of the unblocked and blocked receptors were evaluated with Student's *t* test. Two-way analysis of variance (ANOVA) was used to assess the effects of the different treatments on viability.

## Results and discussion

### Synthesis and chemical characterization

The schematic structure of iPSMA-RGD and its spectroscopic characterization (IR, masses, UV–Vis and HPLC) are shown in Fig. 1. The IR spectrum (Fig. 1B) shows the vibrations from amide I, II and III of the peptide at 1646, 1534 and 1470–1160  $\text{cm}^{-1}$ , respectively. Bands at 1239 and 1161  $\text{cm}^{-1}$ , due to C–N–C vibrations from the DOTA and RGD cycles, are observed. Characteristic bands of the C–N stretch vibration from urea at 1440  $\text{cm}^{-1}$ , related to the iPSMA molecule, is also observed (Fig. 1B). The mass spectrum (Fig. 1C) shows the molecular ion  $[\text{M}+2\text{H}]^{2+}$  at  $m/z = 888.6$  and the ion  $[\text{M}+3\text{H}]^{3+}$  at  $m/z = 592.9$ . Other signals corresponding to the iPSMA-RGD structure as result of fragmentation pattern of the molecule (ionized fragments) are observed at 535.2 (CO- $\beta$ -naphthyl-Ala-Lys-Urea-Glu), 728.9 [cRGDfK(MP)] and 815.0 (cRGDfK(MP-S- $\text{CH}_3$ ))  $m/z$ . The UV spectrum (Fig. 1D) of iPSMA-RGD conjugate shows a band at 269 nm, which is a displacement of approximately 8 nm from the iPSMA and cRGDfK UV-spectra, which showed a characteristic band at  $277 \pm 0.5$  nm. The HPLC chromatogram indicated a chemical purity of > 98% (Fig. 1E). The radiochemical purities of  $^{177}\text{Lu}$ -iPSMA-RGD was  $98.8 \pm 1.0\%$ , as obtained by reversed-phase HPLC ( $n > 12$ ).  $^{177}\text{Lu}$ -iPSMA and  $^{177}\text{Lu}$ -RGD also showed radiochemical purities of > 98%.

### In vitro evaluation and cell studies

$^{177}\text{Lu}$ -iPSMA-RGD was highly stable in human serum since, after 1 and 24 h, only 2 and 6% of the radiopharmaceutical was bound to plasma proteins (shift to higher molecular weight), respectively. Only negligible peaks were eluted at lower molecular weights, indicating that  $^{177}\text{Lu}$ -iPSMA-RGD is not significantly catabolized in serum and therefore has suitable metabolic stability. These results agree with previous studies in which the average fraction of intact radio-RGD or radio-iPSMA ( $^{68}\text{Ga}$ -DOTA-RGD and  $^{111}\text{In}$ -DOTA-RGD or  $^{99\text{m}}\text{Tc}$ -EDDA/HYNIC-iPSMA) in blood is over 85% [2, 16].

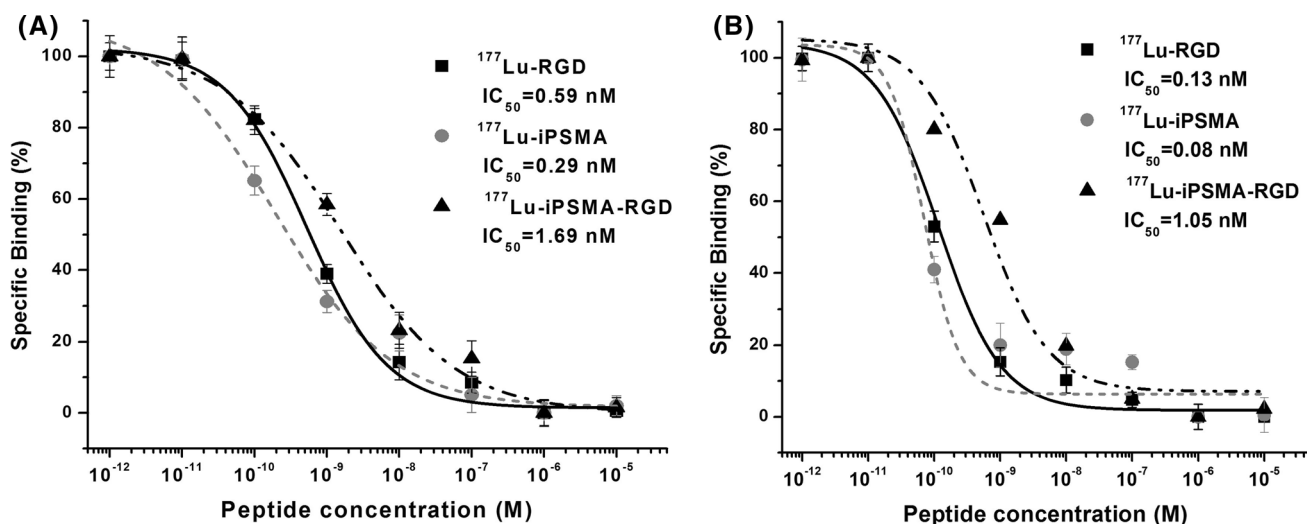
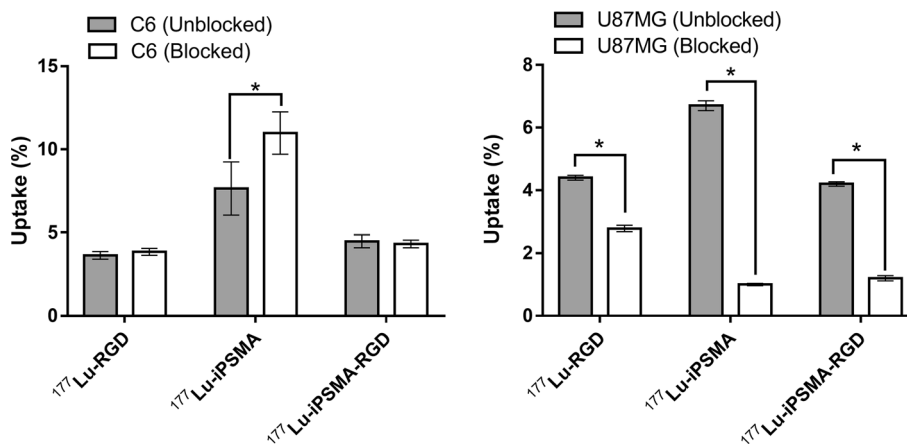


**Fig. 2** Competition assay of a constant concentration of  $^{177}\text{Lu}$ -iPSMA-RGD,  $^{177}\text{Lu}$ -iPSMA, and  $^{177}\text{Lu}$ -RGD with “cold” peptides (iPSMA and/or RGD) at 8 different concentrations (from 10,000 to 0.01 nM in **A** C6 and **B** U87MG cells

**Fig. 3** Specific uptake of  $^{177}\text{Lu}$ -iPSMA-RGD,  $^{177}\text{Lu}$ -iPSMA, and  $^{177}\text{Lu}$ -RGD in C6 and U87MG cells. Cells with blocked receptors were co-incubated with an excess of the respective “cold” peptides (iPSMA-RGD, iPSMA or RGD)



Competition and saturation binding assays were conducted to determine the affinity of  $^{177}\text{Lu}$ -iPSMA-RGD by calculating the  $\text{IC}_{50}$ ,  $K_d$ , and  $B_{\text{max}}$  values. As can be observed in Figs. 2 and 3 and Table 1,  $^{177}\text{Lu}$ -iPSMA-RGD was specifically recognized by PSMA and  $\alpha(v)\beta(3)$  integrins with a suitable affinity (U87MG cells:  $\text{IC}_{50} = 1.05$  nM,  $K_d = 5.81$  nM,  $B_{\text{max}} = 0.32$  nM) to be used as a potential radiotherapeutic radiopharmaceutical. Furthermore, the heterobivalent conjugate also demonstrated the ability to affect significantly ( $p < 0.01$ ) U87MG

and C6 cell viability (Fig. 4). However,  $^{177}\text{Lu}$ -iPSMA and  $^{177}\text{Lu}$ -RGD were found to have a slightly greater affinity for PSMA and integrins than  $^{177}\text{Lu}$ -iPSMA-RGD (Table 1, Fig. 2 and Fig. 3), although with  $\text{IC}_{50}$ ,  $K_d$  and  $B_{\text{max}}$  values in the same order of magnitude for all radiopharmaceuticals. That means that all of them could be useful in targeted radionuclide therapy.

The ANOVA results also indicated that all radioligands had a significant effect ( $p < 0.01$ ) on U87MG and C6 cell viability without statistically significant difference among the three treatments (Fig. 4). Nevertheless, a greater effect on viability was observed in the U87MG cells ( $\sim 30\%$  at 48 h) with regard to C6 ( $\sim 80\%$  at 48 h). Of concern is the apparent non-specific cell uptake of radiopharmaceuticals in C6 cells (Fig. 3), in which blocked cells showed a significant radioactivity uptake. However, the specific binding for all radioligands to C6 cells is evident in the affinity assay results (Fig. 2 and Table 1). This fact could be explained based on the concentration of unlabeled peptides

**Table 1** Affinity of  $^{177}\text{Lu}$ -iPSMA-RGD,  $^{177}\text{Lu}$ -iPSMA, and  $^{177}\text{Lu}$ -RGD, as determined by the saturation assay

Radiotracer	C6 cells		U87MG cells	
	$K_d$ (nM)	$B_{\text{max}}$ (nM)	$K_d$ (nM)	$B_{\text{max}}$ (nM)
$^{177}\text{Lu}$ -RGD	4.54	0.219	4.31	0.366
$^{177}\text{Lu}$ -iPSMA	3.89	0.067	3.84	0.383
$^{177}\text{Lu}$ -iPSMA-RGD	4.60	0.284	5.81	0.321

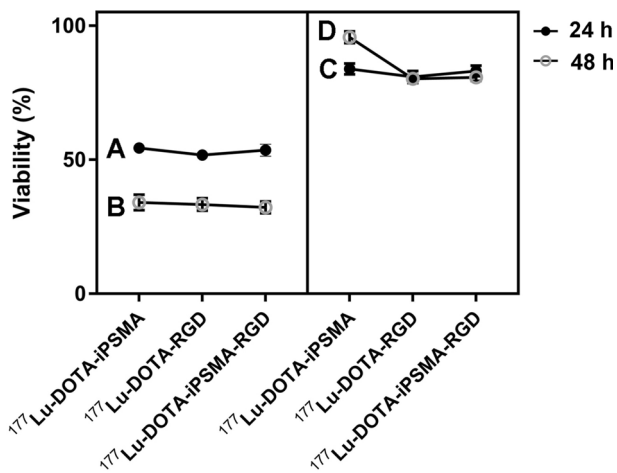


**Fig. 4** Two-way ANOVA results of the radiopharmaceutical's effect on cell viability: *A* U87MG cells after 24 h, *B* U87MG cells after 48 h, *C* C6 cells after 24 h and *D* C6 cells after 48 h. The cells without treatment (control +) represents the 100% of viability. The cells treated with  $^{177}\text{LuCl}_3$  (control-) represents the unspecific uptake subtracted from the treatments

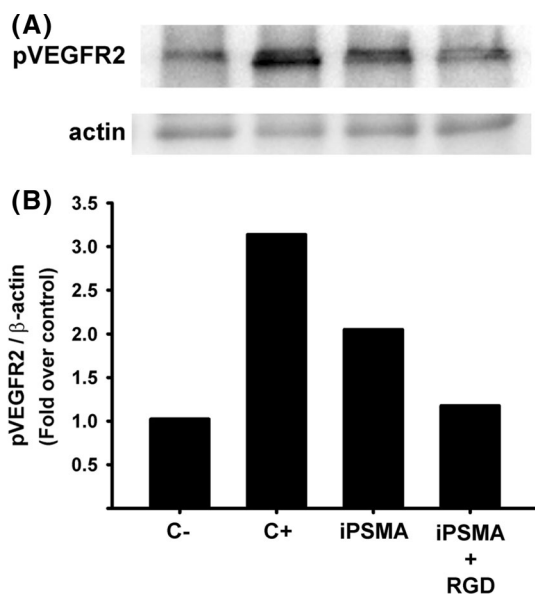


**Fig. 5** **A** Western blot showing phosphorylated VEGFR2 (pVEGFR2, upper panel) and actin (lower panel) performed with previously hypoxic (CoCl<sub>2</sub> 200 μM, 3 h) EA.hy926 cells cultivated in the presence of iPSMA or iPSMA-RGD concomitantly with serum during 5 min. Culture medium without and with serum was used as negative and positive control (C- and C+, respectively). **B** Densitometric analysis of pVEGFR2 normalized against actin is shown in graphical form. Figure represents one experiment

used for the competition/blocking receptors since for the cell uptake test a concentration of 250 μM “cold” peptide was used, while for saturation assays it was two orders of magnitude lower (2 μM). Therefore, the high levels of

“cold” peptide possibly trigger C6 cell mechanisms that promote  $^{177}\text{Lu}$ -peptide internalization, instead of a receptor blocking effect.

Affinity, cell uptake, and viability assays indicated that  $^{177}\text{Lu}$ -iPSMA-RGD was not able to concomitantly recognize two receptors on the cell surface or to improve the cell uptake concerning  $^{177}\text{Lu}$ -iPSMA or  $^{177}\text{Lu}$ -RGD monomers, as other authors have reported for heterobivalent molecules [11–13]. However, the intrinsic heterogeneity of human tumors, as well as changes in phenotype during disease progression, including the different level expression of cell surface receptors, is well-known. Therefore, the use of  $^{177}\text{Lu}$ -iPSMA-RGD as a dual targeting radiopharmaceutical may improve detection sensitivity and therefore, absorbed radiation doses during therapy. Furthermore, heterobivalent molecules may display synergic properties such as enhancement of the antiangiogenic potential. As can be seen in Fig. 5, on hypoxic-like condition iPSMA-RGD was able to inhibit the phosphorylation of VEGFR2 (low pVEGFR2 value) behavior that was not observed with the iPSMA treatment. Therefore, the iPSMA-RGD heterodimeric compound showed suitable properties to act over tumor vasculature as an antiangiogenic molecule [17, 18].

Considering that  $\alpha v \beta 3$  integrin and PSMA are overexpressed in the neovasculature of primary tumors and in metastatic lesions, a synergistic or dual recognition in vivo effect of the  $^{177}\text{Lu}$ -iPSMA-RGD by different solid tumors is expected.

## Conclusions

$^{177}\text{Lu}$ -iPSMA-RGD was prepared with radiochemical purities of > 98%, as a stable and specific radiopharmaceutical to target PSMA and  $\alpha(v) \beta(3)$  integrins, and with suitable affinity to be used as a radiotherapeutic agent. The iPSMA-RGD heterobivalent molecule showed potential to inhibit the VEGFR2 signaling. Nevertheless, preclinical studies are necessary to evaluate and determine the therapeutic potential of  $^{177}\text{Lu}$ -iPSMA-RGD.

**Acknowledgements** This research was carried out as part of the activities of the “Laboratorio Nacional de Investigación y Desarrollo de Radiofármacos, (Mexican National Council of Science and Technology, CONACyT-CB-2016-01-281526)”.

## References

- Santoni M, Scarpelli M, Mazzucchelli R, Lopez-Beltran A, Cheng L, Cascinu S, Montironi R (2014) Targeting prostate-specific membrane antigen for personalized therapies in prostate cancer: morphologic and molecular backgrounds and future promises. *J Biol Regul Homeost Agents* 28(4):555–563

2. Ferro-Flores G, Luna-Gutiérrez M, Ocampo-García B, Santos-Cuevas C, Azorín-Vega E, Jiménez-Mancilla N, Orocio-Rodríguez E, Davanzo J, García-Pérez FO (2017) Clinical translation of a PSMA inhibitor for  $^{99m}\text{Tc}$ -based SPECT. *Nucl Med Biol* 48:36–44
3. Kratochwil C, Giesel FL, Stefanova M, Benešová M, Bronzel M, Afshar-Oromieh A, Mier W, Eder M, Kopka K, Haberkorn U (2016) PSMA-targeted radionuclide therapy of metastatic castration-resistant prostate cancer with  $^{177}\text{Lu}$ -labeled PSMA-617. *J Nucl Med* 57(8):1170–1176
4. Rajasekaran AK, Anilkumar G, Christiansen JJ (2005) Is prostate-specific membrane antigen a multifunctional protein? *Am J Physiol Cell Physiol* 288(5):C975–C981
5. Schwenck J, Tabatabai G, Skardelly M, Reischl G, Beschoner R, Pichler B, La Fougère C (2015) In vivo visualization of prostate-specific membrane antigen in glioblastoma. *Eur J Nucl Med Mol Imagin* 42(1):170
6. Verburg FA, Krohn T, Heinzel A, Mottaghy FM, Behrendt FF (2015) First evidence of PSMA expression in differentiated thyroid cancer using [sup 68 Ga] PSMA-HBED-CC PET/CT. *Eur J Nucl Med Mol Imagin* 42(10):1622
7. Zeng C, Ke Z-F, Yang Z, Wang Z, Yang S-C, Luo C-Q, Wang L-T (2012) Prostate-specific membrane antigen: a new potential prognostic marker of osteosarcoma. *Med Oncol* 29(3):2234–2239
8. Sathegke M, Modiselle M, Vorster M, Mokgoro N, Nyakale N, Mokaleng B, Ebenhan T (2015) 68 Ga-PSMA imaging of metastatic breast cancer. *Eur J Nucl Med Mol Imagin* 42(9):1482–1483
9. Haubner R, Decristoforo C (2009) Radiolabelled RGD peptides and peptidomimetics for tumour targeting. *Front Biosci* 14:872–886
10. Luna-Gutiérrez M, Ferro-Flores G, Ocampo-García B, Jiménez-Mancilla N, Morales-Avila E, León-Rodríguez D, Isaac-Olivé K (2012)  $^{177}\text{Lu}$ -labeled monomeric, dimeric and multimeric RGD peptides for the therapy of tumors expressing  $\alpha(v)\beta(3)$  integrins. *J Label Comp Radiopharm* 55(4):140–148
11. Shallal HM, Minn I, Banerjee SR, Lisok A, Mease RC, Pomper MG (2014) Heterobivalent agents targeting PSMA and integrin- $\alpha v \beta 3$ . *Bioconjug Chem* 25(2):393–405
12. Zhang J, Niu G, Lang L, Li F, Fan X, Yan X, Yao S, Yan W, Huo L, Chen L (2017) Clinical translation of a dual integrin  $\alpha v \beta 3$ -and gastrin-releasing peptide receptor-targeting PET radiotracer, 68 Ga-BBN-RGD. *J Nucl Med* 58(2):228–234
13. Eder M, Schäfer M, Bauder-Wüst U, Haberkorn U, Eisenhut M, Kopka K (2014) Preclinical evaluation of a bispecific low-molecular heterodimer targeting both PSMA and GRPR for improved PET imaging and therapy of prostate cancer. *Prostate* 74(6):659–668
14. Coin I, Beyermann M, Bienert M (2007) Solid-phase peptide synthesis: from standard procedures to the synthesis of difficult sequences. *Nat Protoc* 2(12):3247–3256
15. Ocampo-García BE, Santos-Cuevas CL, De Leon-Rodríguez LM, García-Becerra R, Ordaz-Rosado D, Luna-Gutiérrez MA, Jiménez-Mancilla NP, Romero-Pina ME, Ferro-Flores G (2013) Design and biological evaluation of (9)(9mTc-N(2)S(2)-Tat(49-57)-c(RGDyK): a hybrid radiopharmaceutical for tumors expressing  $\alpha(v)\beta(3)$  integrins. *Nucl Med Biol* 40(4):481–487
16. Decristoforo C, Gonzalez IH, Carlsen J, Rupprich M, Huisman M, Virgolini I, Wester H-J, Haubner R (2008) 68 Ga-and  $^{111}\text{In}$ -labelled DOTA-RGD peptides for imaging of  $\alpha v \beta 3$  integrin expression. *Eur J Nucl Med Mol Imagin* 35(8):1507–1515
17. Chen TT, Luque A, Lee S, Anderson SM, Segura T, Iruela-Arispe ML (2010) Anchorage of VEGF to the extracellular matrix conveys differential signaling responses to endothelial cells. *J Cell Biol* 188(4):595–609
18. Reynolds AR, Hart IR, Watson AR, Welti JC, Silva RG, Robinson SD, Da Violante G, Gourlaouen M, Salih M, Jones MC, Jones DT, Saunders G, Kostourou V, Perron-Sierra F, Norman JC, Tucker GC, Hodivala-Dilke KM (2009) Stimulation of tumor growth and angiogenesis by low concentrations of RGD-mimetic integrin inhibitors. *Nat Med* 15(4):392–400